Organic tandem and multi-junction solar cells

Hadipour, Afshin; de Boer, Bert; Blom, Paul W. M.

Published in:
Advanced Functional Materials

DOI:
10.1002/adfm.200700517

Publication date:
2008

ADVANCED FUNCTIONAL MATERIALS

DOI: 10.1002/adfm.200700517

Organic Tandem and Multi-Junction Solar Cells**

By *Afshin Hadipour*, *Bert de Boer*,* and *Paul W. M. Blom*

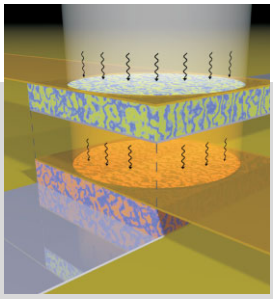

The emerging field of stacked layers (double- and even multi-layers) in organic photovoltaic cells is reviewed. Owing to the limited absorption width of organic molecules and polymers, only a small fraction of the solar flux can be harvested by a single-layer bulk heterojunction photovoltaic cell. Furthermore, the low charge-carrier mobilities of most organic materials limit the thickness of the active layer. Consequently, only part of the intensity of the incident light at the absorption maximum is absorbed. A tandem or multi-junction solar cell, consisting of multiple layers each with their specific absorption maximum and width, can overcome these limitations and can cover a larger part of the solar flux. In addition, tandem or multi-junction solar cells offer the distinct advantage that photon energy is used more efficiently, because the voltage at which charges are collected in each subcell is closer to the energy of the photons absorbed in that cell. Recent developments in both small-molecule and polymeric photovoltaic cells are discussed, and examples of photovoltaic architectures, geometries, and materials combinations that result in tandem and multi-junction solar cells are presented.

1. Introduction

In the last decades, solar cells (converting sunlight into electricity) have attracted much attention as a proper candidate for the main energy source in the future. To produce low-cost and large-area solar cells, many new device structures and materials are being developed. Photoconductivity and electroluminescence were reported in organic crystals, such as anthracene, for the first time in the 1950s.[1–4] The first highly conductive polymer, chemically doped polyacetylene, was reported in 1977.[5] Since then, organic molecules and semiconducting polymers are being increasingly used in (opto)electronic devices. In the last years, the use of organic materials as active layer in photovoltaic devices has attracted more and more attention, and the total conversion efficiency of those cells has increased rapidly.[6–9] First, small (low-molecular-weight) organic molecules[10,11] and later also semiconducting polymers[12,13] were incorporated into solar cells. In general, illumination of an organic semiconductor leads to the creation of excitons[14] with a binding energy of about 0.4 eV[15–17], instead of free charges. The exciton can be separated when it reaches the interface between suited donor (D) and acceptor (A) materials, where the difference in the electron affinities and the ionization potentials between those two (A and D) materials are sufficiently large to overcome the exciton binding energy. The hole and electron are still bound by Coulomb interactions across the D/A interface, even though the opposing charges reside in different organic materials. After breaking the Coulomb binding between the electron in the acceptor and the hole in the donor the electrons and holes are transported through the acceptor and donor phase, respectively, to the electrodes of the device. The transport is assisted by a driving force that is given by the potential difference between the cathode and the anode of the device. However, the low mobility of electrons and holes, together with relatively narrow absorption spectra of the organic materials, leads to a relatively low performance of the organic solar cells. The efficiency typically amounts to 4–5 %, which limits them for practical applications. Excellent reviews have appeared in literature regarding these so-called single-active-layer or mono-junction solar cells.[8,9,18–22] To improve the absorption of the solar radiation by organic solar cells, materials with a broad absorption band have to be designed and produced, or different narrow-band absorbers have to be stacked or mixed in multiple junctions.[11] When two (or more) donor materials with non-overlapping absorption spectra are used in a tandem (or multi-junction) solar cell, a broader range of the solar spectrum (whole visible and part of the IR range) can be covered. Several approaches for organic tandem (multiple) cells have been reported in the last years, depending on the materials used for the active layer and the proper separa-

[*] Dr. B. de Boer, Dr. A. Hadipour, Prof. P. W. M. Blom
Molecular Electronics, Zernike Institute for Advanced Materials
University of Groningen
Nijenborgh 4, 9747 AG Groningen (The Netherlands)
E-mail: b.de.boer@rug.nl

[**] The authors gratefully acknowledge the co-workers at the University of Groningen and their collaborators at the Technical University of Eindhoven, the Energy research Centre of the Netherlands (ECN), and the University of Hasselt (Belgium). Financial supports from the Dutch Polymer Institute (DPI), Netherlands Agency for Energy and Environment (SenterNovem), Foundation for Fundamental Research on Matter (FOM), and the Zernike Institute for Advanced Materials are gratefully acknowledged.

tion or recombination layer(s). All layers can be different in each architecture or approach. In general, the multiple organic solar cells can be divided in three classes:

A) Tandem (or multi-junction) organic solar cells in which low-molecular-weight molecules are used for both the bottom (front) and the top (back) cells

B) Hybrid tandem organic solar cells in which the bottom cell is processed from polymers by solution-processing while the top cell is made of vacuum-deposited low-molecular-weight molecules

C) Fully solution-processed tandem or multi-junction organic solar cells in which both the bottom and the top cells are made of polymers

An overview of the chemical structures of organic materials presently used in organic tandem and multi-junction solar cells is given in Figure 1. Depending on which kinds of materials are being used for the active layers, different separating layers are fabricated and reported. In the following sections, the different types of organic tandem and multi-junction photovoltaic cells are described and recent results obtained by various groups are presented.

2. Tandem and Multilayer Organic Solar Cells Based on Low-Molecular-Weight Molecules

The main advantage of using low-molecular-weight or small molecules for tandem structures is that different layers of donor and acceptor (or mixed layers) materials can be evaporated (or co-evaporated) with sharp interfaces on top of each other, without affecting the already existing layers. A disadvantage of such structures is the relatively low evaporation rate of active

Bert de Boer (April 11, 1973, Peize, The Netherlands) received his M.Sc. degree (1996) and Ph.D. degree (2001) from the University of Groningen (The Netherlands). His Ph.D. thesis, under the supervision of Prof. Georges Hadziioannou, was entitled "Design, Synthesis, Morphology and Properties of Semiconducting Block Copolymers for Photonic Applications". In 2001 he was awarded the TALENT-fellowship from the Netherlands National Science Foundation (NWO) and joined Bell Laboratories of Lucent Technologies (Murray Hill, NJ, USA) as a post-doc to work on molecular electronics based on self-assembled monolayers with Dr. Zhenan Bao. In 2003 he was appointed tenure-track assistant professor "Molecular Electronics" at the Zernike Institute for Advanced Materials of the University of Groningen. His research interests include self-assembled monolayers, molecular electronics, organic photovoltaic devices, organic field-effect transistors, sensors, organic light-emitting diodes, (conjugated) block copolymers, and supramolecular organization.

Afshin Hadipour (October 14, 1968, Abadeh, Iran) received his M.Sc. degree (2003) from the University of Groningen (The Netherlands). His Ph.D. thesis, under the supervision of Dr. Bert de Boer and Prof. Paul Blom, is entitled: "Solution-Processed Tandem Organic Solar Cells". After receiving his Ph.D. degree in December 2007, he will join the Interuniversitair Micro-Electronica Centrum (IMEC) in Belgium as senior researcher.

Paul W. M. Blom received his Ir. degree in Physics (1988) and his Ph.D. degree (1992) from the Technical University Eindhoven (The Netherlands). Joining Philips Research Laboratories in 1992, he was engaged in the electrical characterization of various oxidic thin-film devices, the electro-optical properties of polymer light-emitting diodes, and the field of rewritable optical storage. In May 2000 he was appointed Full Professor at the University of Groningen, where he is leading a group in the field of electrical and optical properties of organic semiconducting devices. At present the main research focus is on the device physics of polymeric light-emitting diodes, transistors, solar cells, and molecular electronics.

ADVANCED FUNCTIONAL MATERIALS

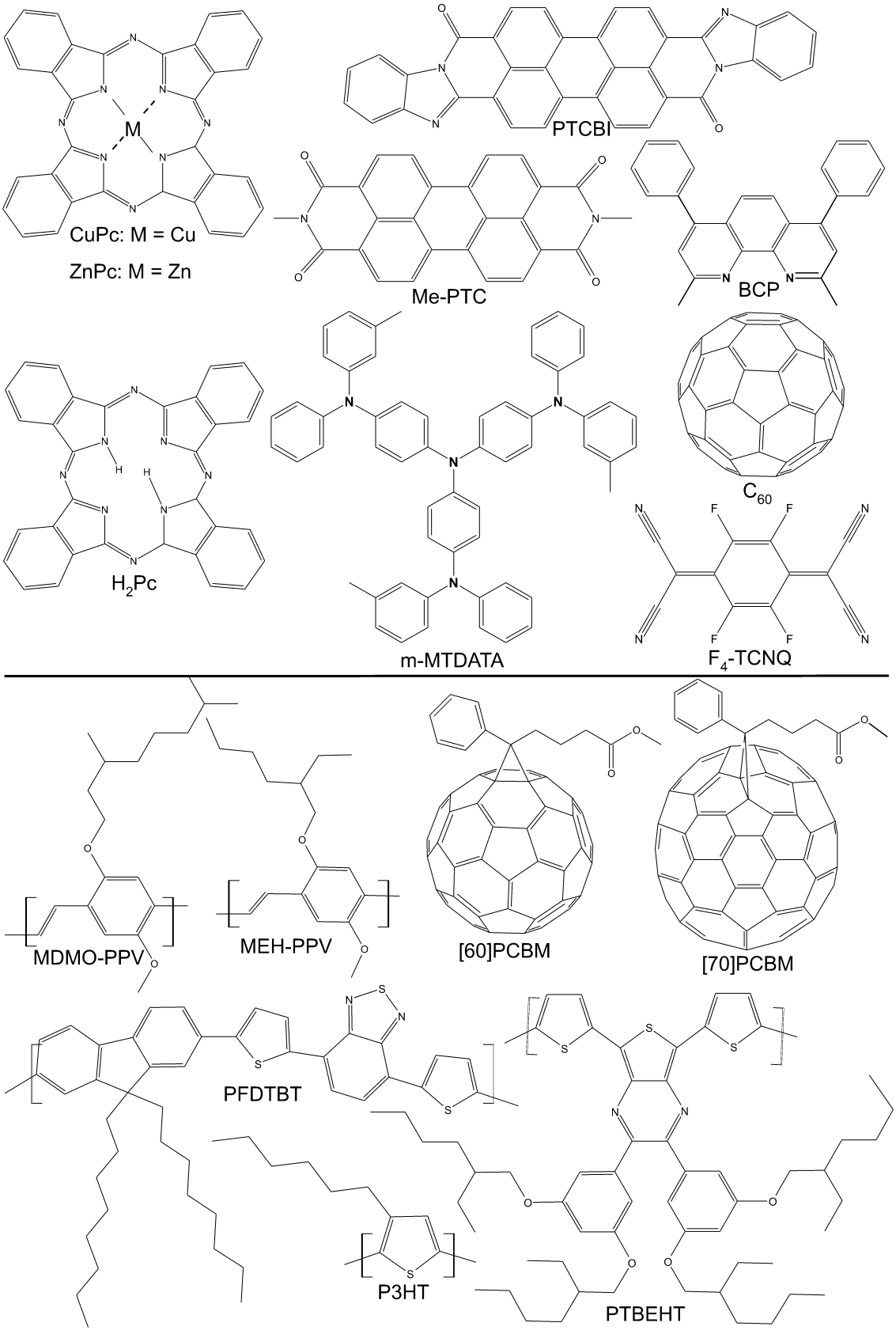

Figure 1. The chemical structures of the donor and the acceptor materials used in organic tandem and multi-junction solar cells. The molecules above the solid line are frequently used in multi-junction photovoltaic cells fabricated by vapor deposition, whereas the polymers and molecules depicted below the solid line are used in solution-processed multi-junction solar cells.

materials, which limits the processing speed for large-area applications. The first organic tandem (double-junction) cell was realized by Hiramoto, Suezaki, and Yokoyama and was constructed from two identical bilayers.[23] Each bilayer consisted of H_2-phthalocyanine (50 nm) and a perylene tetracarboxylic derivative (70 nm) and the two bilayer cells were separated by a thin interstitial layer (2 nm) of Au. This first organic tandem solar cell resulted in almost a doubling of the open-circuit voltage (V_{OC}) to 0.78 V.

Yakimov and Forrest presented the first multiple-heterojunction solar cells by stacking two, three, or five vacuum-deposited ultrathin organic bilayer photovoltaic cells in series.[24] All single thin heterojunction cells[25] (bottom and top cell) are made of Cu-phthalocyanine (CuPc) as a donor and 3,4,9,10-perylene-tetracarboxylic bis-benzimidazole (PTCBI) as an acceptor. The device is processed on an indium tin oxide (ITO) substrate covered by 30 nm poly(ethylenedioxythiophene):polystyrenesulfonic acid (PEDOT:PSS), which serves as anode of the device. The sub-cells are deposited by thermal evaporation in vacuum of ~10^{-6} Torr, starting with the donor material (CuPc) and followed by the acceptor material (PTCBI). A thin layer of silver clusters (0.5 nm) is deposited between the two sub-cells as recombination layer and finally 80 nm Ag is thermally deposited for the cathode of the device. Generally, the built-in voltage of a single heterojunction cell is given by the difference in the Fermi levels of the donor and the acceptor materials used.[26] This means that for a well-performing tandem cell, consisting of two (or more) series-connected heterojunction single cells, the open-circuit voltage of the tandem cell should be equal to the sum of the built-in voltages of the individual cells. However, deposition of the sub-cells in series without a separation layer in between them will cause the formation of an inverse heterojunction between the donor layer of the top (back) cell and the acceptor of the bottom (front) cell. Yakimov and Forrest have placed a very thin and discontinuous layer of silver (0.5 nm Ag) between each sub-cell. The Ag clusters then serve as charge recombination sites. The electrons and the holes arriving from the bottom and the top cell, respectively, can recombine at this separating layer. The structure of the small molecule tandem cell is shown in Figure 2.

After absorption of the incident light in such a structure, excitons are created in both the donor (D) and acceptor (A) material. Only excitons that are created very close (in rang of the exciton diffusion length, ~10 nm)[8,27] to the D/A interface can be separated into charges. Then, the electrons and the holes travel through the acceptor (PTCBI) and donor (CuPc) layers, respectively, to the contacts of the device. The holes of the bottom cell and the electrons of the top cell are extracted from the device, whereas the electrons of the bottom cell recombine with the holes of the top cell at the metallic interlayer (Ag nanoclusters). It was demonstrated that for a thickness of about 11 nm for the donor and also 11 nm for the acceptor layer (22 nm heterojunction) the open-circuit voltage (V_{OC}) and short-circuit current (J_{SC}) are maximized.[24] The V_{OC} and J_{SC} of the tandem cell with two stacked sub-cells and varying thickness for the metallic interlayer (Ag) are summarized in Table 1.

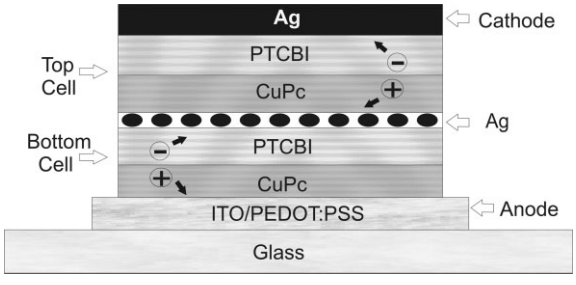

Figure 2. The structure of an organic tandem solar cell based on the small molecules CuPc (donor) and PTCBI (acceptor), as described earlier. [24]. The 0.5 nm Ag separation layer provides recombination sites for the free charges arriving from the bottom and top cell.

Table 1. Data extracted from Ref. [24]: For a Ag interlayer with a thickness of 0.5 nm, the tandem cell has the highest V_{OC} and J_{SC}. For a thinner Ag interlayer, both open-circuit voltage and short-circuit current drop. For a thicker Ag interlayer the V_{OC} has the same values while J_{SC} drops.

Ag thickness [nm]	0	0.5	1.5	3
V_{OC} [V]	0.45	0.9	0.9	0.9
J_{SC} [A m^{-2}]	26	63	52	39

As the data in Table 1 show, the use of a thicker Ag interlayer leads to a much lower photocurrent while the V_{OC} is the same. The high absorption coefficient of the silver interlayer leads to a reduction of the light intensity at the top cell, and therefore the top cell generates a lower current for thicker Ag interlayer. The sub-cells are connected in series, meaning that the current of the tandem cell is limited by the lower current of the two sub-cells, which is the top cell. With the same donor and acceptor materials, Yakimov and Forrest also demonstrated three- and five-fold heterojunction solar cells measured at different light intensities. A summary of their results of V_{OC} and power conversion efficiency (η) of different cells under 1 and 10 sun illuminations is given in Table 2.

To explain the results mentioned above we have to note that the total current extracted from the tandem structure is directly dependent on how efficient charges can recombine at the metallic interlayer (0.5 nm Ag). All sub-cells have to generate the same amount of photocurrent (current matching), since they are connected in series. If one of the individual cells generates much more current than the other(s), charges will pile-up at the very thin Ag interlayer such that the effective bias of the

Table 2. The open-circuit voltage (V_{OC}) and power conversion efficiency (η) of single and multilayer cells under different light intensities are extracted from Ref. [24]. Under 1 sun illumination condition, the dual structure (tandem cell) has the best performance. At higher light intensity of 10 sun, the triple cell reaches the highest efficiency.

Stack cells:	V_{OC} [V] (1 sun)	V_{OC} [V] (10 sun)	η [%] (1 sun)	η [%] (10 sun)
Single cell	0.45	0.43	1.0	0.5
Tandem cell	0.90	0.90	2.5	1.8
Triple cell	1.20	1.40	2.3	2.6
Fivefold cell	1.23	1.70	1.0	1.4

ADVANCED FUNCTIONAL MATERIALS

sub-cells will be far off from their best performance. In addition, in a single bilayer heterojunction cell the excitons must be generated sufficiently close to the D/A interface in the range of L_D ~10 nm[27] such that exciton dissociation can take place. Therefore, the performance of organic bilayer devices is limited by their exciton diffusion length (L_D ~10 nm), which is much shorter than the thickness needed to absorb all incident light (L_A ~150 nm). Stacking of cells in a tandem structure is the way to overcome this limitation. A problem that remains when three or five identical cells are stacked is that under 1 sun illumination the absorption of light by the first two sub-cells leads to a reduction of the photocurrent of the following cells, limiting the total current extracted from the whole device. At higher light intensity (10 sun), the triple cell (instead of the tandem cell) shows the maximum efficiency, but again the light intensity is decreased for the following sub-cells limiting the performance of the complete five-layer (penta-junction) device. Similar experiments using CuPc and PTCBI in combination with ultrathin Ag and Au interlayers were performed by Triyana and co-workers to produce tandem and triple junction solar cells.[28]

To improve the efficiency of stacked solar cells, Xue and Forrest applied several modifications to the structure of the device mentioned above.[29] First, they used C_{60} as acceptor since it has a longer exciton diffusion length of L_D ~40 nm as compared to the previous acceptor PTCBI.[30] Secondly, they incorporated a mixed donor–acceptor layer (bulk heterojunction) sandwiched between pure donor and pure acceptor layers. The homogenous layers of C_{60} and PTCBI serve as electron transport layer (ETL) and hole transport layer (HTL), respectively. The device is called hybrid planar-mixed heterojunction (PM-HJ) device.[29,31] Instead of a very thin Ag interlayer for the recombination sites (separating layer between two sub-cells), they used Ag nanoclusters with a typical thickness of 0.5 nm but buried in a 5 nm thick 4,4′,4”-tris(3-methyl-phenyl-phenyl-amino)triphenylamine (m-MTDATA), which was p-doped with 5 mol % tetrafluoro-tetracyano-quinodimethane (F_4-TCNQ).[29] The reason for using an additional layer of p-doped m-MTDATA is not explained by the authors. Clearly, advantages are found when using doped transport layers, namely:[32,33] doping of this interlayer increasing the conductivity of this layer and reduces ohmic losses, quenching processes at the electrode are avoided since excitons created in the active layer cannot enter the wide-gap transport layer, the thickness of the highly conductive interlayer can be tuned to optimize the optical field distribution in the solar cell, and the increase in overall thickness of the devices allows higher stability and a lower probability for short circuiting the device. It has to be noted that silver particles also serve as scattering centers for incident light. The scattering of light in the middle of the device improves the optical absorption of the active layers of the sub-cells. Finally, thin layers of bathocuproine (BCP)[30,34] and 3,4,9,10-perylenetetracarboxylic bis-benzimidazole (PTCBI) are used as the exciton-blocking layer (EBL) in the top (back) sub-cell and bottom (front) sub-cell, respectively. The structure of the whole device is depicted in Figure 3.

The exciton blocking layers (EBL) serve in three different ways: i) for the top cell it prevents damage of the active layer

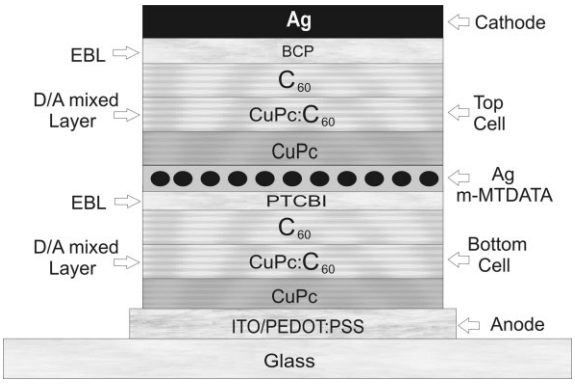

Figure 3. The complete stacked structure of PM-HJ tandem organic solar cell, as described elsewhere [29].

caused by evaporation of a (hot) metallic cathode (hot Ag particles); ii) it also eliminates diffusion of Ag particles, which act as exciton quenching sites, into the active layer; and iii) the EBL layers provide an optical spacer between the active layer and the reflecting cathode of each sub-cell.

In this way, the light intensity can be tuned to be maximized at the D/A interface (or at the mixed donor–acceptor layer), which leads to an improved optical absorption in these devices. Because of the low thicknesses of the active layers (limited by short exciton diffusion length) optical interference between transmitted light through the active layer of the device and the reflected light at cathode of the device has a significant effect on the total absorption of each sub-cell. By using different thicknesses for the active layers, the optical profiles can be tuned inside the device. The donor material CuPc absorbs incident light between 550 nm and 750 nm wavelength, while the acceptor material C_{60} absorbs between 350 nm and 550 nm. Using a thicker homogeneous CuPc layer and thinner homogeneous C_{60} layer in the bottom cell as compared to the top cell (keeping the thickness of mixed donor–acceptor layer fixed), the absorption of the bottom cell is shifted to longer wavelengths relative to the absorption of the top cell. Such an asymmetric absorption of both sub-cells leads to an improved spectral overlap with the sunlight. For current matching, the thicknesses of the homogeneous layers of CuPc and C_{60} and mixed layers have to be further optimized. It is also important to realize that molecular intermixing (mixed layer of each sub-cell) leads to significantly lower charge carrier mobilities compared to those in polycrystalline homogeneous layers (CuPc and C_{60} layers), whereas the exciton separation efficiency is much higher in the mixed layer as compared to pure CuPc or C_{60} layers. The power conversion efficiencies of PM-HJ tandem cells using different thicknesses for the active regions are summarized in Table 3. All thicknesses are in nanometers, beginning with the bottom cell followed by the top cell.

3. Hybrid Tandem Organic Solar Cell

To improve the optical absorption of a single organic solar cell, Dennler and co-workers have stacked a solar cell made of

Table 3. Layer thicknesses in nanometers and efficiencies (%) of various PM-HJ tandem organic solar cells from Ref. [29]. The effect of thickness variations for the active layers is shown. Cell 2 has the best performance because the thicknesses used are the best tradeoff between the electrical and optical properties.

Cell	CuPc	CuPc:C_{60}	C_{60}	PTCBI	CuPc	CuPc:C_{60}	C_{60}	BCP	η [%]
1	10	18	2	5	2	13	25	7.5	5.4
2	7.5	12.5	8	5	6	13	16	7.5	5.7
3	9	11	0	5	5	10	21	10	5.0

the small molecules zinc phthalocyanine:C_{60} (ZnPc:C_{60}) on top of a heterojunction polymer solar cell based on a mixed layer of poly(3-hexylthiophene) (P3HT) and [6,6]-phenyl C_{61}-butyric acid methyl ester (PCBM).[35] For the two sub-cells two different classes of materials (low-molecular-weight molecules and polymer) were used, and these require different processing techniques, namely vapor deposition and spin coating. Therefore, this structure is called a hybrid tandem organic solar cell. The tandem cell is processed onto ITO-coated glass covered by a 90 nm thick layer of PEDOT:PSS. A layer (clusters) of 1 nm gold (Au) is used as intermediate layer between the two sub-cells, which serves as a recombination center. The P3HT polymer is dissolved in chlorobenzene and PCBM is dissolved in dichloromethane. The layer of P3HT is spin-coated first, followed by spin-coating of the PCBM layer. This structure is called a diffused bilayer,[35] or stratified bilayer.[36] The rest of the device is processed by thermal evaporation under vacuum (10^{-6} mbar). First, 10 nm C_{60} is evaporated serving as electron transport layer (ETL) for the bottom cell. Then, 1 nm Au is evaporated to enhance the recombination of hole and electrons from the top and bottom cell, respectively. The top cell is subsequently fabricated by thermal evaporation of 10 nm of zinc phthalocyanine (ZnPc), 40 nm of a mixture of ZnPc and C_{60}, and 15 nm of C_{60}. The device is completed by evaporation of 5 nm of chromium and 95 nm of aluminum, which acts as the cathode of the device. In this way, the bottom cell is not affected or damaged during the processing of the top cell. The structure of the device is shown in Figure 4.

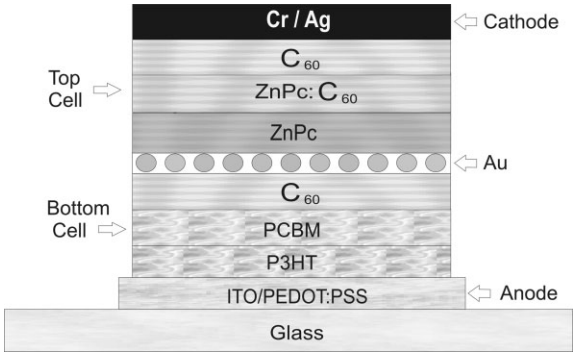

Figure 4. The structure of a hybrid tandem organic solar cell. The top cell, made of small molecules, is evaporated on top of the bottom cell based on a diffused bilayer of the conjugated polymer P3HT and the fullerene PCBM, which is processed from solution.

To compare the performance of the tandem cell with the single sub-cells, Dennler and co-workers have also processed two reference single cells. They used ITO/P3HT:PCBM/Al processed as diffused bilayer as a reference for the bottom cell and ITO/ZnPc/ZnPc:C_{60}/C_{60}/Cr/Al as a reference for the top cell. The bottom cell has its main absorption between 375 and 630 nm, while the top cell mainly absorbs in the range of 600 to 800 nm. As a result, the tandem cell covers the whole visible range of the solar spectrum (from 400 to 800 nm). The measured performance of the tandem device and reference sub-cells under 1 sun simulated light are summarized in Table 4.

Table 4. Performance of the hybrid tandem organic solar cell [35]. The performance of the tandem cell is compared with the reference bottom and the reference top cells.

Cell	J_{SC} [A m^{-2}]	V_{OC} [V]	FF [%]	η [%]
Ref. Bottom	85	0.55	55	2.6
Ref. Top	93	0.47	50	2.2
Tandem	48	1.02	45	2.3

The results in Table 4 confirm the successful coupling of the two sub-cells in series using the 1 nm Au recombination layer, since the V_{OC} of the tandem cell is equal to the sum of the V_{OC} of the bottom and the top cell. However, the performance of the tandem cell is limited by the lower photocurrent and fill factor (FF) extracted from the device. The thicknesses of the active layers of the sub-cells are not yet optimized. Also the photocurrent of the tandem, reference bottom, and reference top cells were measured under monochromatic light as a function of wavelength. By using monochromatic incident light the *J–V* characteristics of each individual sub-cell can be measured and compared with the performance of the tandem cell, as summarized in Table 5.

Table 5. The J_{SC} of the tandem cell, reference bottom and reference top cell measured under monochromatic light with different wavelength [35].

Cell	J_{SC} [mA W^{-1}] λ = 500 nm	J_{SC} [mA W^{-1}] λ = 600 nm	J_{SC} [mA W^{-1}] λ = 700 nm
Ref. Bottom	138	120	10
Ref. Top	32	100	110
Tandem cell	8	51	2

Table 5 demonstrates that the tandem cell is only efficient when both sub-cells perform properly. If one of the individual cells generates a low current, the current extracted from the tandem device is limited due to the series connection. As mentioned above, the main advantage of hybrid tandem organic solar cells is the absence of solvents for the processing of the top cell since the top cell has to be vapor-deposited. However, using both processing methods may lead to higher costs of producing tandem (multiple) solar cells for commercial applications.

ADVANCED FUNCTIONAL MATERIALS

4. Solution-Processed Tandem Organic Solar Cells

Semiconducting polymers are appropriate materials for developing low-cost technologies for large-area solar cells, because polymers can be deposited from solution using simple methods such as spin-coating and ink-jet printing.[37,38] The main problem in the fabrication of polymer tandem cells is the stack integrity: deposition of the top cell might dissolve or damage the earlier deposited bottom cell, especially when similar solvents as chlorobenzene and chloroform are used. Therefore, a separating layer (middle contact) is required that has to be thick enough (a closed layer) to protect the bottom cell from dissolving during spin coating (processing) of the top cell. At the same time, the middle contact has to be as transparent as possible to transmit light efficiently to the top cell. To overcome the stack integrity problem different structures and methods have been reported recently, which are discussed in the following sections.

4.1. Tandem Organic Solar Cell Processed on Separated Substrates

One of the methods to overcome the processing difficulties is reported by Shrotriya and co-workers.[39] Two identical bulk heterojunction single cells were fabricated onto different glass substrates and then positioned on top of each other. The sub-cells are connected in series or in parallel outside the device. The bottom cell has a semitransparent cathode consisting of 1 nm thick LiF, 2.5 nm Al, and 12.5 nm Au with a maximum transparency of about 74 % at 580 nm. Both sub-cells are fabricated from a blend of poly(2-methoxy-5-(2′-ethyl)-hexyloxy)-1,4-phenylene vinylene (MEH-PPV) and PCBM with a 1:4 weight ratio. The thickness of the active layer of both the bottom and the top cell is about 70 nm. For PPV-based solar cells it is known that an increase of the active layer thickness does lead to an increased absorption, but not to an increased performance.[40] The absorption increase is cancelled by increased space-charge formation and recombination. Using two thin identical active layers for both sub-cells is an attempt to effectively increase the absorption while maintaining the favorable electrical properties of thin devices. However, the coverage of the solar spectrum is not improved. The structure of the device from reference [39] is given in Figure 5. Furthermore, various semitransparent cathodes have been investigated. The highest transparency and best performance was obtained with the above-mentioned LiF/Al/Au cathode. Finally, it should be noted that the efficiency of ca. 2.5 % of both the parallel and series tandem cell is equal to the efficiency of a single layer device with a thickness of 140 nm. Apparently, the coupling of two identical thin cells does not bring advantage as compared to a single cell with the same total active layer thickness. Shrotriya and Yang have connected the sub-cells in series and in parallel. They have compared the performance of the bottom, the top, and the connected devices (series and parallel) under 1 sun simulated solar light. A summary of their results is given in Table 6.

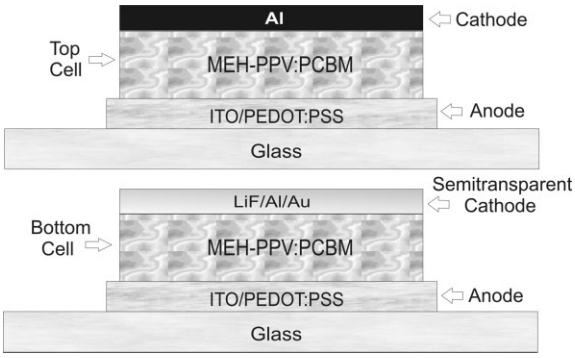

Figure 5. The separated sub-cells positioned on top of each other, as described in Ref. [39]. The bottom cell has a semitransparent cathode.

Table 6. Performance of stacked organic solar sell processed on separated substrates [39]. For the measurements of the devices connected in series and in parallel, the bottom cell was positioned in front of the top cell, allowing the light to transmit through the bottom cell before reaching the active layer of the top cell.

Cell	V_{OC} [V]	J_{SC} [A m^{-2}]	FF [%]	η [%]
Bottom	0.86	26	45	1.1
Top	0.86	32	45	1.3
Series connected	1.64	34	45	2.4
Parallel connected	0.84	63	45	2.5

4.2. Tandem Organic Solar Cell with ITO as Separating Layer

Another polymer based tandem cell is reported recently by Kawano and co-workers. Two bulk heterojunction solar cells were electronically coupled with a interlayer of ITO.[41] The stacked bulk heterojunction solar cells (BHJ) are both based on a 80 nm blend of poly[2-methoxy-5-(3′,7′-dimethyloctyloxy)-1,4-phenylene vinylene] (MDMO-PPV) and PCBM (1:4 weight ratio). As the separating layer, Kawano and co-workers deposited ITO by dc magnetron sputtering in 1 Pa of argon gas without substrate heating. The presence of argon gas into the deposition chamber prevents damaging of the active layer of the bottom cell during deposition of the ITO layer. The full structure of the device is given in Figure 6.

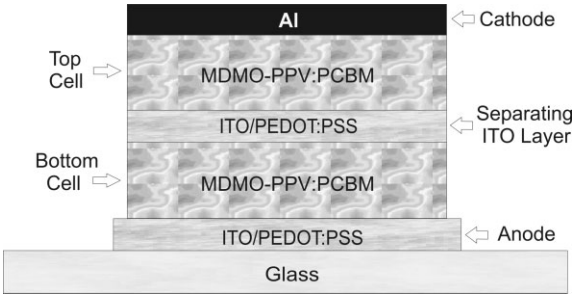

Figure 6. The structure of tandem cell, as fabricated in Ref. [41]. The two sub-cells are separated by a layer of ITO.

The most important aspect of this report is the method used to sputter the ITO onto the polymer surface without damaging it. The very high transparency of the ITO layer enhances the light intensity reaching the top cell resulting in an increased photocurrent of the top cell. A summary of the results achieved by the authors using a 20 nm ITO interlayer is given in Table 7.

Table 7. Performance of a tandem organic solar cell with 20 nm ITO as separating layer [41]. The performance of the tandem cell is compared to a reference BHJ single cell (using a ITO/PEDOT/80 nm MDMO-PPV:PCBM/Al structure).

Cell	V_{OC} [V]	J_{SC} [A m^{-2}]	FF [%]	η [%]
Reference	0.84	46	59	2.3
Tandem	1.34	41	56	3.1

As the data of Table 7 demonstrate, connection of the two sub-cells in series leads in this case to a V_{OC} of 1.6 times higher than the reference cell, instead of the double value. The reason is that the high work function of ITO (~4.8–5.0 eV) will limit the maximum V_{OC} of the bottom cell.[42] Thus, the absence of an ohmic contact for electron extraction at the interface between the separating layer and the active layer of the bottom cell (lowest unoccupied molecular orbital (LUMO) of the PCBM in the blend) leads to a decrease of the V_{OC} of the bottom cell from 0.84 V (normal value when using an ohmic contact) to 0.48 V, leading to a V_{OC} of the tandem cell of 1.28 V. Since in this study the same donor material (MDMO-PPV) is used for both sub-cells the narrow absorption of the active layer is not improved. However, optimizing this structure using a transparent, low-work-function, metallic layer between the bottom cell and the ITO interlayer, in combination with donor materials with non-overlapping absorption band can lead to the fabrication of highly efficient tandem cells.

4.3. Tandem Organic Solar Cell with Composite Metallic Interlayers

The first solution-processed organic tandem solar cell consisting of two bulk heterojunction sub-cells with complementary absorption spectra is presented by Hadipour and co-workers.[43] The two sub-cells are separated by a composite middle electrode mainly based on metals. In order to harvest as many photons of the solar spectrum as possible, a high band-gap donor material poly((2,7-(9,9-dioctyl)-fluorene)-*alt*-5,5-(4,7-di-2-thienyl-2,1,3-benzothiadiazole) (PFDTBT)[44,45] for the bottom cell is combined with a low-band-gap polymer poly{5,7-di-2-thienyl-2,3-bis(3,5-di(2-ethylhexyloxy)phenyl)-thieno[3,4-*b*]pyrazine} (PTBEHT)[46] for the top cell. The fullerene derivative PCBM is used as acceptor material for both sub-cells. As a result, the photons with higher energy are absorbed in the bottom cell, whereas the transmitted lower energy photons are absorbed by the top cell. The absorption spectra of the donor materials used in this tandem structure are given in Figure 7.

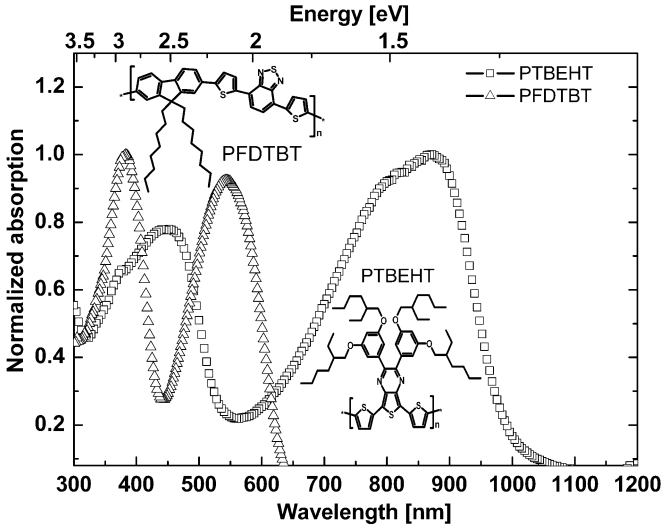

Figure 7. The absorption spectra of the large band gap donor material PFDTBT used in the bottom cell together with the absorption spectra of the small band gap polymer PTBEHT used in the top cell. The sub-cells have complementary absorption maxima at 550 nm for PFDTBT and 850 nm for PTBEHT.

To compare bottom, top, and the tandem cell performances in the same device at the same time, we used identical contacts for the devices. The combination of Au/PEDOT:PSS is used for the anode of the device while LiF/Al is used as the cathode of the device. The middle contact here serves three different purposes: as a charge recombination center, as a protecting layer for the bottom cell during spin coating of the top cell, and as semitransparent mirror that creates an optical cavity which allows for tuning of the transmission of the solar flux through the bottom cell. The sub-cells are electrically coupled together in series, which results in a V_{OC} of the tandem cell that equals the sum of the V_{OC} of each sub-cell. The structure of the tandem cell is given in Figure 8.

Figure 8. The structure of a solution-processed tandem organic solar cell as processed in Ref. [43]. The two bulk heterojunction sub-cells are connected in series by the semitransparent middle contact. The absorptions of the sub-cells are complementary.

The active layer of the bottom cell acts as dielectric, sandwiched between two semitransparent layers (between the anode and the middle contact of the bottom cell). In such a geom-

ADVANCED FUNCTIONAL MATERIALS

etry transmitted light through the active layer interferes with the reflected light at the middle contact, which leads to optical cavities.[47–49] The transmitted light through the bottom cell is thus affected by the thickness of its active layer. Therefore, the optical transmission through the bottom cell can be tuned to match the maximum absorption of the top cell. Figure 9 demonstrates that for a thickness of 110 nm PFDTBT:PCBM blend (1:4) for the bottom cell, the transmitted light is at its maximum at 850 nm wavelength (dark triangle in Fig. 9). This is the optimum thickness for the active layer of the bottom cell since the top cell absorbed mainly between 700 and 950 nm (Fig. 7).

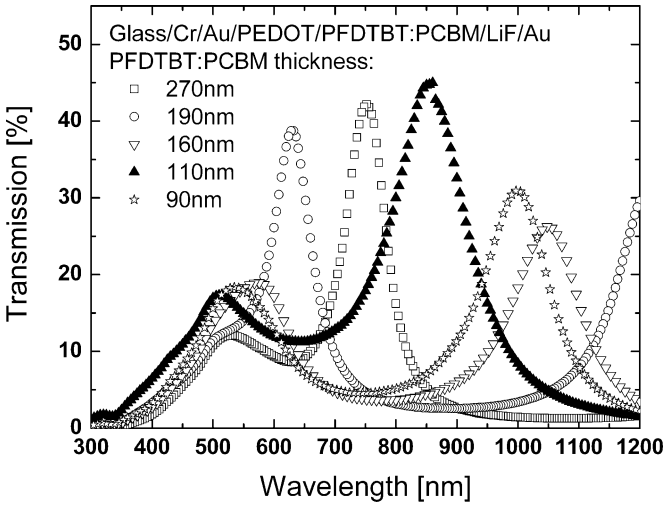

Figure 9. The optical transmission through the bottom cell for different thicknesses of the active layer of the device. At thickness 110 nm, the transmission matches the absorption of the top cell at 850 nm.

The middle contact serves as cathode of the bottom cell and in the same time as anode of the top cell. A thin layer of 0.5 nm LiF/0.5 nm Al (work function ~3.7 eV) is used to match the LUMO of PCBM and acts as cathode of the bottom cell. A layer of 60 nm PEDOT:PSS (work function ~5.2 eV) is used to stabilize the work function of the middle gold electrode and to match the highest occupied molecular orbital (HOMO) of the donor PTBEHT used in the top cell (anode of the top cell). The PEDOT:PSS also improves the wetting for the processing of the active layer of the top cell. The current extracted from the tandem cell follows the lowest of the currents generated in the bottom and top cell, since two sub-cells are stacked in series. The optimum thickness of the top cell is about 90 nm. The combination of the above-mentioned materials and thicknesses leads to an optimized optical and electrical matching of the tandem cell. The results of the final device are given in Figure 10.

As the data of Figure 10 demonstrate, both sub-cells generate the same amount of photocurrent. The complementary absorption band of the donor materials used for each sub-cell (PFDTBT and PTBEHT) leads to coverage of the whole visible range of the solar spectrum. The performance of the tandem cell, as extracted from Figure 10, is 1.6 times higher than

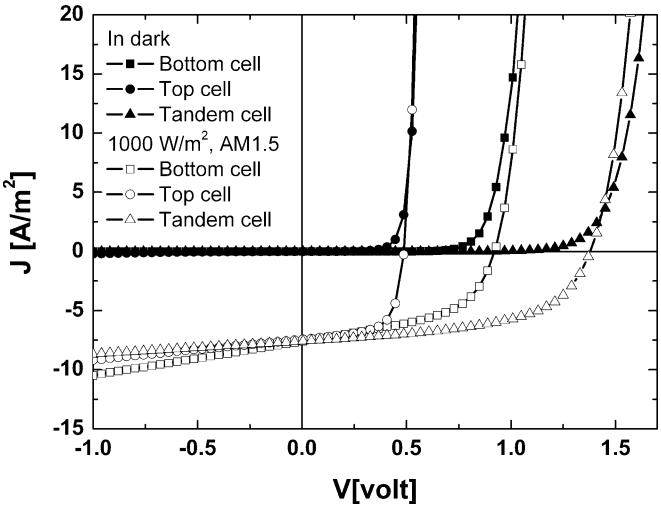

Figure 10. The current–voltage (*J–V*) measurements of the bottom, top and tandem cell. The *J–V* of the bottom cell is measured by using anode and the middle contact (cathode of the bottom cell) as depicted in Figure 8. The *J–V* of the top cell is measured by using the middle contact (anode of the top cell) and cathode in Figure 8. The *J–V* of the tandem cell is measured by using anode and cathode in Figure 8.

the performance of the bottom cell and 2.5 times higher as compared to the performance of the top cell.

4.4. Tandem Solar Cells with Optical Spacer as Interlayers

As mentioned in Section 4.3, the layer thickness of the bottom cell had to be optimized in such a way that the optical output coupling is adapted to the absorption of the top cell. A disadvantage of this approach is that the optimum thickness of the bottom cell, required to match the optical output, is not necessarily equal to the thickness at which the bottom cell reaches its optimum electrical performance. If, for example, a thickness of 300 nm is required for optical out coupling the occurrence of unbalanced transport may lead to the formation of space-charges, giving rise to a reduced fill factor and performance.[40,42,50–53] To circumvent this limitation we introduced an additional solution-processable, transparent, and insulating layer which serves as an optical spacer and leads to the fabrication of a four-contact tandem cell.[54] In this second-generation tandem cell, the thickness of the bottom cell is first optimized for its electrical performance. Then, the optical output coupling is tuned by varying the thickness of the optical spacer on top of the bottom cell. The transmitted light through the complete stack of the bottom solar cell with the optical spacer is matched with absorption spectrum of the small-band-gap polymer of the top cell. Since the optical spacer is an insulator, the fabrication of tandem cells with four electrodes is feasible and, consequently, the two sub-cells can be coupled electronically (external) in parallel or in series. All other tandem photovoltaic cells fabricated by sequential processing of layers that are reported in literature so far, are electronically connected in series, owing to the limited in-plane conductivity (high sheet resistance) of the middle electrode (separating layer or recombination layer).

FEATURE ARTICLE

The schematic structure of the second-generation solar cells is given in Figure 11.

As depicted in Figure 11, the two organic solar cells are linked together by an insulating, solution-processable and transparent layer of poly(trifluoroethylene) (PTrFE) dissolved in methyl ethyl ketone (MEK). This spin coated layer acts as an optical spacer to tune the optical out coupling of the bottom

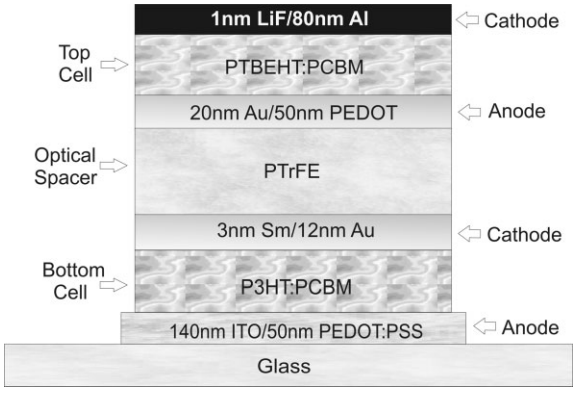

Figure 11. The structure of the second generation tandem cell in which an additional optical spacer is used that allows for independent tuning of the optical cavity. Two bulk heterojunction cells (bottom and top cell) are stacked electronically in series or parallel outside the device (four terminal device). The absorption spectra of the two semiconducting polymers P3HT and PTBEHT are complementary.

cell. Two of the four contacts used here in the tandem configuration are known to be efficient in BHJ solar cells, namely, 140 nm ITO/50 nm PEDOT:PSS as anode for the bottom cell and 1 nm LiF/80 nm Al as cathode of the top cell.[40,42] For the cathode of the bottom cell 3 nm of samarium topped with 12 nm Au was found to be very transparent, highly conductive, and stable during spin-coating of the PTrFE layer. The work function of Sm was found to be low enough (2.7 eV[55]) to provide an ohmic contact with the bottom cell in order to maximize the V_{OC}. On top of the PTrFE optical spacer a bilayer of 20 nm Au and 50 nm PEDOT:PSS was chosen for the anode of the top cell. A layer thickness of at least 20 nm is required to for the Au layer to reach a sufficiently low sheet resistance and the PEDOT:PSS facilitates the processing of the top cell and stabilizes the work function of the anode.

The bottom cell is fabricated from P3HT:PCBM (1:1) according to standard procedures[52] and was found to perform best for a cell with a layer thickness of 250 nm. The thickness of the top cell made of PTBEHT:PCBM (1:4) is kept to 90 nm, which was found to give the best performance.[43,46] After optimization of the layer thickness of the bottom cell, the wavelength of the transmitted light output can now be tuned to match the absorption spectrum of the top cell by varying the thickness of the optical spacer (PTrFE layer). Figure 12 demonstrates that a layer thickness of the optical spacer of 250 nm, in combination with 250 nm P3HT:PCBM/3 nm Sm/12 nm Au, results in an optical out coupling of the bottom stack that matches the absorption of the small band gap polymer

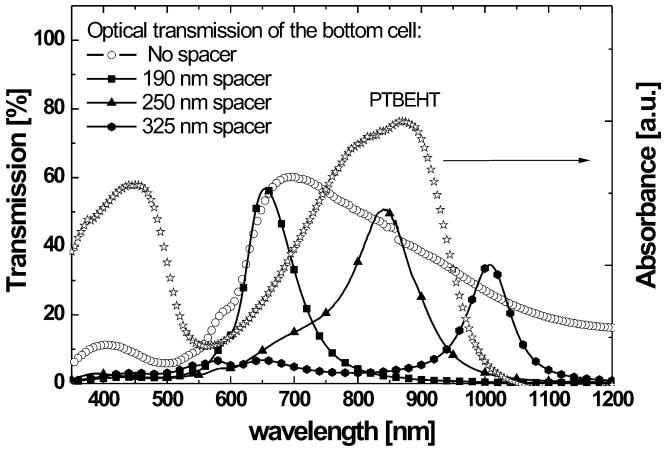

Figure 12. Optical out coupling of incident light through the bottom cell consisting of glass/140 nm ITO/50 nm PEDOT:PSS/250 nm P3HT:PCBM (1:1)/3 nm Sm/12 nm Au/*x* nm PTrFE/20 nm Au/PEDOT:PSS. For a blend of P3HT:PCBM (1:1) with a layer thickness of 250 nm (and no optical spacer), the light output is not yet matched with the absorption of the small band gap polymer of the top cell (700–950 nm). By spin coating an supplementary transparent layer of PTrFE, the transmitted light can be tuned in order to match the absorption of the top cell.

PTBEHT in the top cell. The bottom cell processed from 250 nm P3HT:PCBM (1:1) topped with an optical spacer (PTrFE) of 250 nm transmits about 50 % in the wavelength range that is absorbed by the small band gap polymer PTBEHT.

The *J–V* measurements of the individual bottom and top cells, and of the tandem cell connected in series and parallel are depicted in Figure 13. As expected, the top cell strongly limits the photocurrent of the tandem cell connected in se-

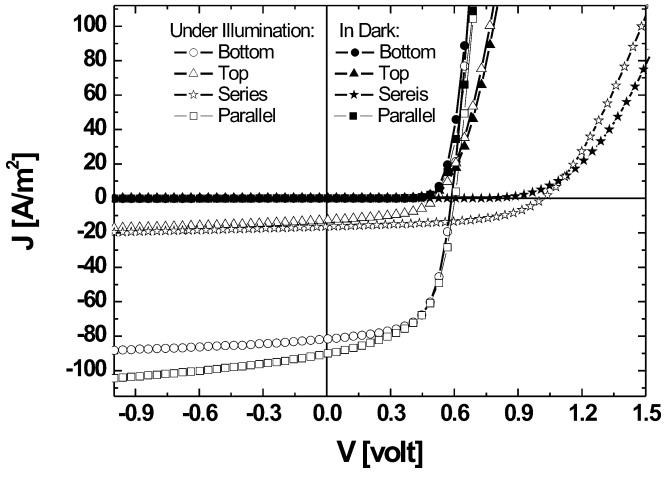

Figure 13. *J–V* characteristics of the bottom and top cell measured separately, and the tandem cells connected in series and in parallel in the dark and under illumination with simulated solar light of 1000 W m^{-2}. In the series configuration, the current density is limited by the lowest current density of the two cells and the V_{OC} is the sum of both sub-cells. In the parallel configuration, the current density is equal to the sum of both sub-cells and the V_{OC} is limited to the lowest V_{OC} of the sub-cells.

ADVANCED FUNCTIONAL MATERIALS

ries.[56] In our four-terminal tandem geometry, the two sub-cells can also be easily connected in parallel. Since the top cell generates a much lower photocurrent as compared to the bottom cell the parallel tandem solar cell leads to a higher performance as compared to the tandem solar cell connected in series.[56] Indeed, the V_{OC} of the parallel tandem cell is close to the V_{OC} of the bottom and top cells, while the current is the sum of both photocurrents generated by the two sub-cells. The series configuration has a high V_{OC} (1.03 V), while its short circuit current (J_{SC} = 16.3 A m^{-2}) is limited by the lower current of the top cell. The parallel configuration shows the same V_{OC} as both sub-cells (0.59 V), combined with a higher J_{SC} (92.0 A m^{-2}). It should be noted that in the present parallel configuration the performance hardly exceeds the performance of the bottom cell alone. Since the current of this tandem cell is equal to the sum of the currents generated by both sub-cells, the lower fill factor (FF) of the top cell (50 %) (compared to the high FF of the bottom cell (64 %)) also affects the fill factor of the tandem cell (54 %).[56] This lower fill factor compensates the gain in photocurrent in the parallel tandem solar cell.

4.5. Multiple Organic Solar Cell with Solution-Processed Interlayers

One of the latest approaches to fully solution-processed organic tandem solar cell is reported by Gilot, Wienk, and Janssen, in which a solution-processed middle electrode (separating layer) is introduced.[57] These kinds of electrodes demonstrate the possibility to realize fully solution-processed solar cells (tandem or multiple cells) without using vapor-deposited contacts. For the fabrication of the separating layer, ZnO nanoparticles were prepared,[58,59] dissolved in acetone, and spin-coated. To create a high-work-function anode, neutral pH PEDOT (ORGACON, pH = 7, 1.2 wt %, Agfa Gevaert NV) was spin-coated from a water-based suspension. The normal acidic PEDOT:PSS can not be used since ZnO layer dissolves in an acidic solution. The ZnO layer serves as electron transporting layer (ETL), while the neutral PEDOT acts as hole transporting layer (HTL). The active layers are fabricated from a chlorobenzene solution of the donor materials MDMO-PPV or P3HT mixed with the acceptor material PCBM in a 1:4 and 1:1 ratio, respectively. The thicknesses of the active layers are 45 nm and 85 nm for the bottom and top cell of the tandem junction and 45 nm, 65 nm, and 85 nm for the bottom, middle, and top cell of the triple junction. The structure of this tandem device is given in Figure 14.

The recombination of the charges across the interface between ZnO and neutral pH PEDOT is normally very poor since a large energy offset exists at the interface between them. An ohmic contact between ZnO and PEDOT is needed to prevent a voltage drop across the interface and allows the holes and the electrons to recombine efficiently. To increase the recombination probability, the two materials have to be sufficiently doped or metallic clusters (0.5 nm Ag or Au) have to be deposited between them. In this study doping methods have been applied: The PEDOT is all p-doped, whereas the doping of the ZnO layer can be reached by exposing the layer to UV light (photo-doping) for a few seconds.[60,61] A summary of their results for tandem and triple solar cells using MDMO-PPV:PCBM for all active layers and photo-doped ZnO/neutral pH PEDOT layer is given in Table 8.

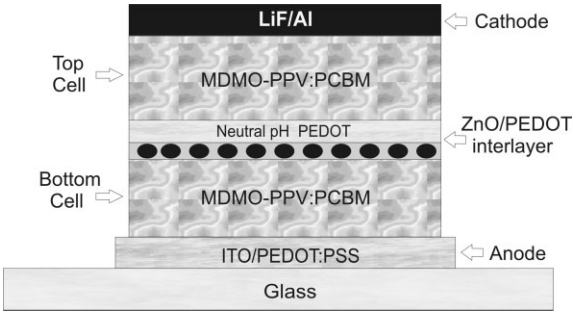

Figure 14. The structure of tandem solar cell based on ZnO/PEDOT as separating layer. The MDMO-PPV:PCBM (1:4) layers are 45 nm and 85 nm thick for the bottom and the top cell, respectively.

Table 8. Performance of multi-junction organic solar cell with a solution-processed interlayer taken from Ref. [57]. The tandem cell has a 45 nm active layer for the bottom and 85 nm layer for the top cell. The triple cell is based on 45 nm, 65 nm, and 85 nm active layers for the bottom, the middle and the top cell, respectively.

Cell	V_{OC} [V]	J_{SC} [A m^{-2}]	FF [%]
Single Cell	0.82	49	57
Tandem Cell	1.53	30	40
Triple Cell	1.92	24	33

As the data of Table 8 demonstrate, the V_{OC} of the multi-junction solar cells connected in series are slightly lower than the sum of the V_{OC} of the individual sub-cells. The deviation of the V_{OC} from estimated values (two or three times the V_{OC} of the single cell) is probably caused by a small voltage drop at the interface between ZnO and neutral pH PEDOT. The very high transparency of the ZnO/PEDOT interlayer in combination with the possibility to fabricate the whole multi-junction solar cell from solution makes this approach very useful and practical for future applications.

4.6. Tandem Organic Solar Cells with Solution-Processed TiO_x Interlayers

The most recent and efficient tandem organic solar cell based on solution processing is reported by Kim et al.[62] In this tandem cell a highly transparent titanium oxide (TiO_x) layer is used to separate the two sub-cells of the tandem device**.** Similar to the approach by Gilot et al.,[57] but now using this transparent TiO_x middle electrode, also fully solution-processed solar cells (tandem or multiple cells) can be realized. The advantages of using oxides such as the above-mentioned ZnO or TiO_x for the middle electrode is the optical transparency of the layer and the orthogonally compatible solvents used for processing

all layers. In these cases, the separating layer does not significantly affect the light intensity. This high light intensity at the top cell leads to a high photocurrent generated by the top cell. Therefore, the efficiency of the tandem device is not limited any more by the lower current of the top cell as observed for tandem structures with metallic interlayer. The cell was processed onto glass/ITO substrate covered by 40 nm thick layer of PEDOT:PSS (Baytron P). The transparent TiO_x interlayer is fabricated by spin coating form methanol solution by means of sol-gel chemistry.[63] For the bottom BHJ cell a 130 nm thick layer of PCPDTBT:PCBM (1:3.6)[64] was used that was processed from chlorobenzene. The top BHJ cell is fabricated from 170 nm thick P3HT:PC_{70}BM (1:0.7) blend which was processed from chloroform. The two sub-cells have complementary absorption spectra, which leads to coverage of the whole visible and part of the infrared spectrum by the tandem device. On top of the TiO_x interlayer layer, the highly conductive hole transport layer PEDOT:PSS (Baytron PH500) was spin coated. The structure of the device is given in Figure 15.

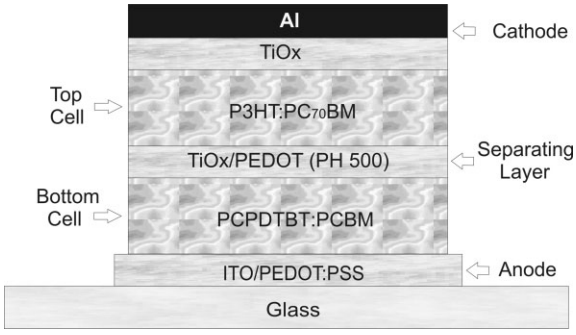

Figure 15. The structure of the tandem device from Ref. [62] is depicted. The two sub-cells are separated by a highly transparent layer of TiO_x covered by the highly conductive PEDOT:PSS (PH 500).

The performance of the above-mentioned tandem device in the dark and under illumination with different light intensities was measured and the results of these measurements are summarized in Table 9.

As listed in Table 9, this all-solution processed tandem cell has the maximum efficiency reported until now of all tandem organic solar cells. The power-conversion efficiency reaches more than 6 % at illuminations of 200 mW cm^{-2}. The main reasons for the high efficiency in this series tandem cell is the relatively high photocurrent of sub-cells caused by using a transparent separating interlayer.

Table 9. The data extracted from Ref. [62]. An optimum tandem solar cell is measured under different light intensities.

Light intensity [W m^{-2}]	200	500	1000	2000
FF [%]	0.68	0.67	0.66	0.64
J_{SC} [A m^{-2}]	24	38	75	150
V_{OC} [V]	1.15	1.2	1.25	1.28
η [%]	6.7	6.5	6.3	6.2

5. Conclusions

In order to achieve organic solar cells with higher performance, the narrowness of the optical absorption of the active layer has to be improved. By using two (or more) donor materials with non-overlapping absorption spectra in a tandem or multi-junction structure, the whole visible range of the solar light can be absorbed and even extended into the near IR. In addition to covering a larger part of the spectrum, tandem solar cells offer the distinct advantage that photon energy is used more efficiently because the voltage at which charges are collected in each sub-cell is closer to the energy of the photons absorbed in that cell. In the various tandem structures the layer that separates both sub-cells plays a very important role. The final efficiency of the tandem cell depends directly on the electrical (ohmic contact and proper conductivity) and optical (transparency) properties of this middle electrode. In the series configuration, the middle contact serves as recombination sites only and therefore does not have to be highly conductive. In the parallel configuration, the sheet-conductivity has to be high since the contact is also used to extract the charges from the device. This overview demonstrates that recently developed multi-junction photovoltaic cells with optimized materials and thicknesses lead eventually to higher efficiencies as compared to single layer solar cells. Recently power-conversion efficiencies of more than 6 % have been achieved using solution-processed organic bulk heterojunction tandem solar cells. The realization of working organic tandem and multi-junction photovoltaic cells is an important step forward to the improvement and finally commercialization of large-area organic solar cells.

Received: May 9, 2007
Revised: October 25, 2007
Published online: January 3, 2008

[1] H. Mette, *Z. Physik* **1953**, *134*, 566.
[2] O. H. Le Blanc, *J. Chem. Phys.* **1960**, *33*, 626.
[3] R. G. Kepler, *Phys. Rev.* **1960**, *119*, 1226.
[4] M. Pope, H. P. Kallmann, P. Magnante, *J. Chem. Phys.* **1963**, *38*, 2042.
[5] C. K. Chiang, C. R. Fincher, Jr., Y. W. Park, A. J. Heeger, H. Shirakawa, E. J. Louis, S. C. Gau, A. G. MacDiarmid, *Phys. Rev. Lett.* **1977**, *39*, 1098.
[6] C. W. Tang, *Appl. Phys. Lett.* **1986**, *48*, 183.
[7] B. A. Gregg, *J. Phys. Chem. B* **2003**, *107*, 4688.
[8] C. J. Brabec, N. S. Sariciftci, J. C. Hummelen, *Adv. Funct. Mater.* **2001**, *11*, 15.
[9] J. Nelson, *Curr. Opin. Solid State Mater. Sci.* **2002**, *6*, 87.
[10] G. A. Chamberlain, *Sol. Cells* **1983**, *8*, 47.
[11] P. Peumans, A. Yakimov, S. R. Forrest, *J. Appl. Phys.* **2003**, *93*, 3693.
[12] G. Yu, J. Gao, J. C. Hummelen, F. Wudl, A. J. Heeger, *Science* **1995**, *270*, 1789.
[13] T. A. Skotheim, R. L. Elsenbaumer, J. R. Reynolds, *Handbook of Conducting Polymers*, Marcel Dekker, New York **1998**.
[14] M. Pope, C. E. Swenberg, *Electronic Processes in Organic Crystals and Polymers*, 2nd ed., Oxford University Press, New York **1999**.
[15] S. Barth, H. Bässler, *Phys. Rev. Lett.* **1997**, *79*, 4445.
[16] P. G. Dacosta, E. M. Conwell, *Phys. Rev. B* **1993**, *48*, 1993.
[17] R. N. Marks, J. J. M. Halls, D. C. Bradley, R. H. Friend, A. B. Holmes, *J. Phys. Condens. Matter* **1994**, *6*, 1379.

ADVANCED FUNCTIONAL MATERIALS

[18] A. Goetzberger, C. Hebling, *Sol. Energy Mater. Sol. Cells* **2000**, *62*, 1.
[19] J.-M. Nunzi, *C. R. Phys.* **2002**, *3*, 523.
[20] D. Wöhrle, D. Meissner, *Adv. Mater.* **1991**, *3*, 129.
[21] H. Spanggaard, F. C. Krebs, *Sol. Energy Mater. Sol. Cells* **2004**, *83*, 125.
[22] K. M. Coakley, M. D. McGehee, *Chem. Mater.* **2004**, *16*, 4533.
[23] M. Hiramoto, M. Suezaki, M. Yokoyama, *Chem. Lett.* **1990**, 327.
[24] A. Yakimov, S. R. Forrest, *Appl. Phys. Lett*. **2002**, *80*, 1667.
[25] P. Peumans, V. Bulovic, S. R. Forrest, *Appl. Phys. Lett*. **2000**, *76*, 2650.
[26] C. W. Tang, *Appl. Phys. Lett.* **1986**, *48*, 183.
[27] a) D. E. Markov, E. Amsterdam, P. W. M. Blom, A. B. Sieval, J. C. Hummelen, *J. Phys. Chem. A* **2005**, *109*, 5266. b) D. E. Markov, J. C. Hummelen, P. W. M. Blom, A. B. Sieval, *Phys. Rev. B* **2005**, *72*, 045216. c) D. E. Markov, *Ph.D. Thesis*, University of Groningen **2006**. Online:http://irs.ub.rug.nl/ppn/296023094.
[28] a) K. Triyana, T. Yasuda, K. Fujita, T. Tsutsui, *Jpn. J. Appl. Phys. Part 1* **2004**, *43*, 2352. b) K. Triyana, T. Yasuda, K. Fujita, T. Tsutsui, *Thin Solid Films* **2005**, *447*, 198.
[29] J. Xue, S. Uchida, B. P. Rand, S. R. Forrest, *Appl. Phys. Lett.* **2004**, *85*, 5757.
[30] P. Peumans, A. Yakimov, S. R. Forrest, *J. Appl. Phys.* **2003**, *93*, 3693.
[31] J. Xue, B. P. Rand, S. Uchida, S. R. Forrest, *Adv. Mater.* **2005**, *17*, 66.
[32] B. Maenning, J. Drechsel, D. Gebeyehu, P. Simon, F. Kozlowski, A. Werner, F. Li, D. Grundmann, S. Sonntag, M. Koch, K. Leo, M. Pfeiffer, H. Hoppe, D. Meissner, N. S. Sariciftci, I. Riedel, V. Dyakonov, J. Parisi, *Appl. Phys. A* **2004**, *79*, 1.
[33] J. Drechsel, B. Männig, D. Gebeyehu, M. Pfeiffer, K. Leo, H. Hoppe, *Org. Electron.* **2004**, *5*, 175.
[34] P. Peumans, V. Bulovic, S. R. Forrest, *Appl. Phys. Lett*. **2000**, *76*, 2650.
[35] G. Dennler, H.-J. Prall, R. Koeppe, M. Egginger, R. Autengruber, N. S. Sariciftci, *Appl. Phys. Lett.* **2006**, *89*, 073502.
[36] L. Chen, D. Godovsky, O. Inganäs, J. C. Hummelen, R. A. J. Janssen, M. Svensson, M. R. Andersson, *Adv. Mater.* **2000**, *12*, 1367.
[37] S. E. Shaheen, R. Radspinner, N. Peyghambarian, G. E. Jabbour, *Appl. Phys. Lett.* **2001**, *79*, 2996.
[38] G. Gustafsson, Y. Cao, G. M. Treacy, F. Klavetter, N. Colaneri, A. J. Heeger, *Nature* **1992**, *357*, 477.
[39] V. Shrotriya, E. H. Wu, G. Li, Y. Yao, Y. Yang, *Appl. Phys. Lett.* **2006**, *88*, 064104.
[40] M. Lenes, L. J. A. Koster, V. D. Mihailetchi, P. W. M. Blom, *Appl. Phys. Lett.* **2006**, *88*, 243502.
[41] K. Kawano, N. Ito, T. Nishimori, J. Sakai, *Appl. Phys. Lett.* **2006**, *88*, 073514.
[42] a) L. J. A. Koster, *Ph.D. Thesis*, University of Groningen **2007**. Online: http://irs.ub.rug.nl/ppn/299329410. b) V. D. Mihailetchi, *Ph. D. Thesis*, University of Groningen **2005**. Online: http://irs.ub.rug.nl/ppn/288520572.
[43] A. Hadipour, B. de Boer, J. Wildeman, F. B. Kooistra, J. C. Hummelen, M. G. R. Turbiez, M. M. Wienk, R. A. J. Janssen, P. W. M. Blom, *Adv. Funct. Mater.* **2006**, *16*, 1897.
[44] M. Svensson, F. Zhang, S. C. Veenstra, W. J. H. Verhees, J. C. Hummelen, J. M. Kroon, O. Inganäs, M. R. Andersson, *Adv. Mater.* **2003**, *15*, 988.
[45] M. Svensson, F. Zhang, O. Inganäs, M. R. Andersson, *Synth. Met.* **2003**, *135–136*, 137.
[46] M. M. Wienk, M. G. R. Turbiez, M. P. Struijk, M. Fonrodona, R. A. J. Janssen, *Appl. Phys. Lett.* **2006**, *88*, 153511.
[47] a) H. Hoppe, N. Arnold, N. S. Sariciftci, D. Meissner, *Sol. Energy Mater. Sol. Cells* **2003**, *80*, 105. b) H. Hoppe, N. Arnold, D. Meissner, N. S. Sariciftci, *Thin Solid Films* **2004**, *451–452*, 589.
[48] D. W. Sievers, V. Shrotriya, Y. Yang, *J. Appl. Phys.* **2006**, *100*, 114509.
[49] A. J. Moulé, K. Meerholz, *Appl. Phys. B* **2007**, *86*, 721.
[50] L. J. A. Koster, V. D. Mihailetchi, R. Ramaker, P. W. M. Blom, *Appl. Phys. Lett*. **2005**, *86*, 123509.
[51] L. J. A. Koster, V. D. Mihailetchi, H. Xie, P. W. M. Blom, *Appl. Phys. Lett*. **2005**, *87*, 203502.
[52] V. D. Mihailetchi, H. Xie, B. de Boer, L. J. A. Koster, P. W. M. Blom, *Adv. Funct. Mater.* **2006**, *16*, 699.
[53] V. D. Mihailetchi, H. Xie, B. de Boer, L. M. Popescu, J. C. Hummelen, P. W. M. Blom, L. J. A. Koster, *Appl. Phys. Lett.* **2006**, *89*, 012107.
[54] A. Hadipour, B. de Boer, P. W. M. Blom, *J. Appl. Phys.* **2007**, *102*, 074506.
[55] *Handbook of Chemistry and Physics*, 75th ed. (Ed: D. R. Lide), CRC Press, Boca Raton, FL **1995**. We have evaporated 20 nm samarium on glass and measured its work function to be 2.4 eV with the Kelvin probe under N_2 atmosphere.
[56] A. Hadipour, B. de Boer, P. W. M. Blom, *Org. Electron.*, in press.
[57] J. Gilot, M. M. Wienk, R. A. J. Janssen, *Appl. Phys. Lett.* **2007**, *90*, 143512.
[58] C. Pacholski, A. Kornowski, H. Weller, *Angew. Chem. Int. Ed.* **2002**, *41*, 1188.
[59] W. J. E. Beek, M. M. Wienk, R. A. J. Janssen, *Adv. Mater.* **2004**, *16*, 1009.
[60] W. J. E. Beek, M. M. Wienk, M. Kemerink, X. Yang, R. A. J. Janssen, *J. Phys. Chem. B* **2005**, *109*, 9505.
[61] F. Verbakel, S. C. J. Meskers, R. A. J. Janssen, *Appl. Phys. Lett.* **2006**, *89*, 102103.
[62] J. Y. Kim, K. Lee, N. E. Coates, D. Moses, T.-Q. Nguyen, M. Dante, A. J. Heeger, *Science* **2007**, *317*, 222.
[63] J. Y. Kim, S. H. Kim, H.-H. Lee, K. Lee, W. Ma, X. Gong, A. J. Heeger, *Adv. Mater.* **2006**, *18*, 572.
[64] D. Mühlbacher, M. Scharber, M. Morana, Z. Zhu, D. Waller, R. Gaudiana, C. Brabec, *Adv. Mater.* **2006**, *18*, 2884.